Phonon-mediated coupling between quantum dots through an off-resonant microcavity

Arka Majumdar,* Michal Bajcsy, Armand Rundquist, Erik Kim, and Jelena Vučković
E. L. Ginzton Laboratory, Stanford University, Stanford, California 94305*, USA*
(Received 21 November 2011; revised manuscript received 19 April 2012; published 1 May 2012)

We present experimental results showing phonon-mediated coupling between two quantum dots embedded inside a photonic-crystal microcavity. With only one of the dots being spectrally close to the cavity, we observe both frequency up-conversion and down-conversion of the pump light via a ∼1.2-THz phonon. We demonstrate this process for both weak and strong regimes of dot-cavity coupling and provide a simple theoretical model to qualitatively explain our observations.

DOI: 10.1103/PhysRevB.85.195301 PACS number(s): 42.50.Pq, 63.20.kk

I. INTRODUCTION

Phonon-mediated coupling between a self-assembled semiconductor quantum dot (QD) and a semiconductor microcavity is a recently discovered phenomenon unique to solid-state cavity quantum electrodynamics. This phenomenon has been observed both in photoluminescence studies under above-band pumping[1–5] and under resonant excitation of the QD.[6,7] The coupling observed via photoluminescence is attributed to several phenomena, including the electron-phonon interactions,[8–13] multiexciton complexes,[14] and charges in the vicinity of the QD.[15] To isolate the role of phonons in off-resonant QD-cavity coupling, studies employing resonant excitation of the QD are preferable as they avoid possible complications arising from multiexcitonic complexes and nearby charges generated via above-band pumping. Apart from the fundamental interest in identifying the mechanism behind this off-resonant coupling,[8–11,14,16] this effect can be used to probe the coherent interaction of the QD with a strong laser[17] as well as the cavity-enhanced AC stark shift of a QD.[18] These results demonstrate that the off-resonant cavity constitutes an efficient readout channel for the QD states.

However, all phonon-assisted off-resonant interaction experiments reported so far in the literature are based on a single QD and a cavity. Recently, an experimental study of two spatially separated QDs interacting resonantly in a microcavity has been reported[19] as well as a theoretical analysis[20–24] of the possible energy-transfer mechanisms between QDs in such a cavity. The interaction between two spectrally detuned QDs via a photonic-crystal cavity has also been demonstrated recently under p-shell QD excitation.[25] However, the actual coupling mechanism between two QDs is not conclusively proven in that experiment as the presence of a higher-energy pumping laser can create charges and multiexcitons, making the system more complex. In our work, we show that under resonant excitation (of one of the dots), two spectrally far-detuned QDs can interact with each other via an off-resonant cavity. More specifically, we observe emission from a spectrally detuned QD when another QD is resonantly excited. Both frequency down-conversion (energy transfer from a higher-energy QD to a lower-energy QD) and up-conversion (energy transfer from a lower-energy QD to a higher-energy QD) are observed for a frequency separation of up to ∼±1.2 THz. Such a large energy difference cannot be ascribed to an excited state of the same QD as opposed to conclusions reached in an earlier work by Flagg *et al.*,[26] which was performed without a cavity and for a frequency difference of ∼±0.2 THz. Based on our observations, we believe this process occurs between two different QDs, and the coupling between the QDs is enhanced by the presence of the cavity.

II. THEORY

The experimental system we want to model is shown in Fig. 1(a). QD1, spectrally detuned from both the cavity and QD2, is resonantly excited with a pump laser. The excitation is transferred to the cavity and QD2 via an incoherent phonon-mediated coupling.[27] We note that, in theory, it is possible to transfer energy directly from QD1 to QD2 via phonons. However, we observe the QD2 emission to be strongly dependent on the QD2-cavity detuning, and hence, the presence of a cavity is important for our experiment. In particular, for detunings greater than a few cavity linewidths, the QD2 emission becomes weak and eventually vanishes.

The master equation used to describe the lossy dynamics of the density matrix ρ of a coupled system consisting of two QDs and a cavity is given by

$$\frac{d\rho}{dt} = -i[\mathcal{H},\rho] + 2\kappa\mathcal{L}[a] + 2\gamma_1\mathcal{L}[\sigma_1] + 2\gamma_2\mathcal{L}[\sigma_2]. \quad (1)$$

Assuming the rotating-wave approximation, the Hamiltonian describing the coherent dynamics of the system $\mathcal{H}$ can be written in the interaction picture as

$$\mathcal{H} = \omega_c a^\dagger a + \omega_{d1}\sigma_1^\dagger\sigma_1 + g_1(a^\dagger\sigma_1 + a\sigma_1^\dagger) + \omega_{d2}\sigma_2^\dagger\sigma_2 + g_2(a^\dagger\sigma_2 + a\sigma_2^\dagger), \quad (2)$$

while the Lindblad operator modeling the incoherent decay via a collapse operator D is $\mathcal{L}[D] = D\rho D^\dagger - \frac{1}{2}D^\dagger D\rho - \frac{1}{2}\rho D^\dagger D$. Additionally, κ is the cavity-field-decay rate; γ_1 and γ_2 are the QD-dipole-decay rates; ω_c, ω_{d1}, and ω_{d2} are the resonance frequencies of the cavity, QD1, and QD2, respectively; and g_1 and g_2 are the coherent-interaction strengths between the cavity and the two QDs, respectively. The resonant driving of QD1 or QD2 can be described, respectively, by adding the term $\Omega(\sigma_1 + \sigma_1^\dagger)$ or $\Omega(\sigma_2 + \sigma_2^\dagger)$ to the Hamiltonian $\mathcal{H}$. The driving-laser frequency is denoted by ω_l. We model the incoherent phonon-mediated coupling by adding $2\gamma_{r1}\mathcal{L}[a^\dagger\sigma_1]$ and $2\gamma_{r2}\mathcal{L}[a\sigma_2^\dagger]$ to the master equation.[27] We note that the phonon-QD-interaction strength depends on the phonon frequency and is, in general, not a constant.[9,10] However, as we are focusing only on a small range of detunings in our

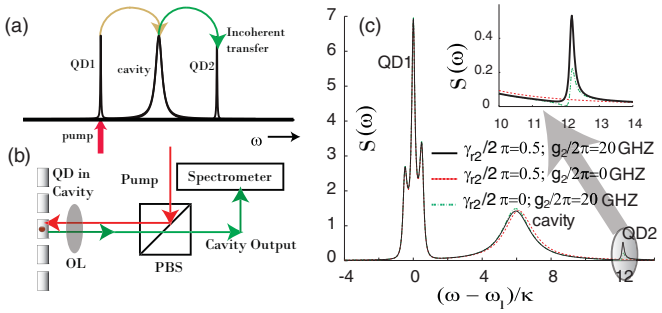

FIG. 1. (Color online) (a) Illustration of the phonon-assisted interdot coupling. QD1 is resonantly driven with a pump laser. The excitation is transferred to QD2 via the cavity. (b) Experimental crosspolarized confocal-microscopy setup with a polarizing-beam splitter (PBS) and an objective lens (OL). (c) Numerically calculated power spectral density $S(\omega)$ of the cavity output for different QD2-phonon-coupling strengths γ_{r2} and QD2-cavity mode coupling g_2. QD1 is resonantly excited (i.e., $\omega_l = \omega_{d1}$), and QD1-cavity coupling is $g_1/2\pi = 20$ GHz while the QD1-phonon-coupling rate is $\gamma_{r1}/2\pi = 0.5$ GHz. The cavity-field-decay rate is $\kappa/2\pi = 20$ GHz. The inset shows a zoom-in of the emission at the QD2 frequency.

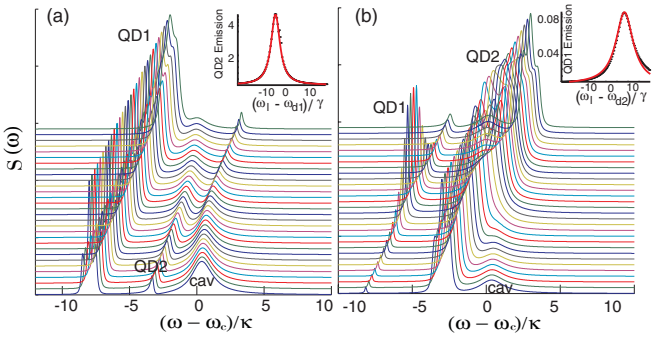

FIG. 2. (Color online) Calculated $S(\omega)$ when (a) QD1 and (b) QD2 are resonantly excited and the dot-cavity detunings are changed. In other words, (a) $\omega_l = \omega_{d1}$, and (b) $\omega_l = \omega_{d2}$. QD1 and QD2 resonances are tuned together as in the experiment. (a) When QD1 is resonantly driven, we observe anticrossing between QD2 and the cavity in the higher-energy off-resonant emission. (b) On the other hand, when QD2 is resonantly driven, we observe an increase in QD1 emission when QD2 is resonant with the cavity. For (a) and (b), parameters used for the simulations were $\gamma_1/2\pi = \gamma_2/2\pi = 1$ GHz, $\gamma_{r1}/2\pi = \gamma_{r2}/2\pi = 0.5$ GHz, $g_1/2\pi = g_2/2\pi = 20$ GHz, $\kappa/2\pi = 20$ GHz, detuning between two dots are 5κ, and driving-laser strength $\Omega_0/2\pi = 5$ GHz. Insets of (a) and (b) show the QD1 and QD2 linewidths measured via monitoring QD2 and QD1 emission, respectively. The simulation result is fit with a Lorentzian to estimate the linewidths.

experiments, a constant rate of QD-phonon interaction can be assumed. The channel between QD1 and the cavity is then characterized by the rates γ_{r1} and g_1 while the channel between the cavity and QD2 is characterized by γ_{r2} and g_2. Figure 1(c) shows the numerically simulated power spectral density (PSD) of the cavity output $S(\omega) = \int_{-\infty}^{\infty} \langle a^\dagger(\tau) a(0) \rangle e^{-i\omega\tau} d\tau$ when the lower-energy QD1 is resonantly driven with a laser. We use only the cavity operator to calculate the PSD because experimentally most of the collected light (even off-resonant) is coupled to the cavity mode. For these simulations, we use $\gamma_1/2\pi = \gamma_2/2\pi = 1$ GHz, $\gamma_{r1}/2\pi = 0.5$ GHz, $g_1/2\pi = 20$ GHz, $\kappa/2\pi = 20$ GHz, QD1-cavity detuning $\Delta_1 = 6\kappa$, QD2-cavity detuning $\Delta_2 = -6\kappa$, and the driving-laser strength $\Omega_0/2\pi = 5$ GHz.

We first study the role of γ_{r2} and g_2 in the QD2 emission. Without g_2, no emission from QD2 is observed; in the presence of g_2, QD2 emission appears, and γ_{r2} enhances it [Fig. 1(c)]. This shows that coherent coupling between the cavity and QD2 is required to observe this dot-to-dot coupling. Although QD2 emission is observed even in the absence of its coupling to phonons (for $\gamma_{r2} = 0$), such emission is much weaker than when a phonon-assisted process is present. The three peaks observed at the QD1 resonance are the usual Mollow triplet, modified due to the presence of the cavity and phonons.[27–29] We note that to observe the off-resonant emissions from the cavity and QD2, we also need to have a phonon-assisted interaction between QD1 and the cavity, i.e., a nonzero γ_{r1}.

Next, we theoretically analyze the dependence of the interdot coupling on the spectral detuning between the undriven dot and the cavity. In an actual experiment, it is very difficult to tune only one QD without affecting the other as the two QDs are spatially very close to each other. Hence, in the simulation, we changed both QD resonances and kept the cavity resonance fixed. In Fig. 2(a) we excite the lower-energy QD1, which is spectrally far detuned from the cavity. QD2 is spectrally close to the cavity and strongly coupled to it. The resonant excitation of QD1 causes light to be emitted both from the cavity and from QD2. Additionally, we observe anticrossing between the cavity and QD2 as the frequency of QD2 is tuned. Following this, we excite the higher-energy QD2 resonantly and observe emission from QD1 [Fig. 2(b)]. We observe an increase in the QD1-emission intensity when QD2 is resonant with the cavity. We note that we always calculate $S(\omega)$ from the autocorrelation of the cavity-field operator and that the emission from QD1(2) is, respectively, the value $S(\omega_{d1})$ and $S(\omega_{d2})$. Finally, we calculate the linewidth of QD1 while measuring the emission from QD2 [inset of Fig. 2(a)] as well as the linewidth of QD2 while measuring the emission from QD1 [inset of Fig. 2(b)] for a weak-excitation-laser power ($\Omega_0/2\pi = 1$ GHz). The dotted black points are the simulation results, and we fit a Lorentzian to estimate the linewidth. We find that the linewidth of QD1 is 4 GHz, and the linewidth of QD2 is 9 GHz. These simulated linewidths are larger than the linewidths one would expect based on just the decay rates, i.e., $2(\gamma + \gamma_r)/2\pi = 3$ GHz; this results from the presence of the cavity and from power broadening induced by the driving laser.[27] However, the linewidths of the QDs are much smaller than that of the cavity (linewidth of 40 GHz), showing that the coupling is indeed between the two QDs. We note that the slight shifts in the measured QD resonances from the bare QD resonances ω_{d1} and ω_{d2} arise from a dispersive shift caused by the cavity.

III. EXPERIMENT: TEMPORAL DYNAMICS OF DOT-CAVITY OFF-RESONANT COUPLING

In this section, we describe an experiment to estimate the time required to transfer the energy from a QD to the cavity when the QD is resonantly excited. This measurement gives a way to estimate the incoherent-coupling rate γ_r.

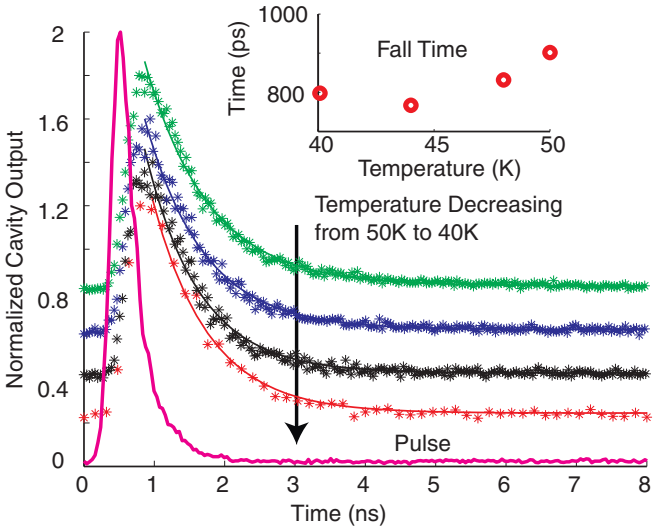

FIG. 3. (Color online) Time-resolved measurement of the off-resonant cavity emission. The QD is resonantly excited with a 40-ps pulse, and the time-resolved measurement of the higher-energy off-resonant cavity emission is performed. The inset plots the fall times of the cavity emission (extracted from the exponential fits) against the system's temperature.

The experiments are performed in a helium-flow cryostat at cryogenic temperatures (∼30–55 K) on self-assembled InAs QDs embedded in a GaAs three-hole defect L_3 photonic-crystal cavity.[30] The 160-nm GaAs membrane used to fabricate the photonic crystal is grown by molecular-beam epitaxy on top of a GaAs (100) wafer. The GaAs membrane sits on a 918-nm sacrificial layer of $Al_{0.8}Ga_{0.2}As$. Under the sacrificial layer, a 10-period distributed Bragg reflector consisting of a quarter-wave AlAs/GaAs stack is used to increase the signal collection into the objective lens. The photonic crystal was fabricated using electron-beam lithography, dry plasma etching, and wet etching of the sacrificial layer.[30]

We resonantly excite the QD with a laser-pulse train consisting of ∼40-ps-wide pulses with a repetition period of 13 ns. A grating filter is used to collect only the off-resonant cavity emission (at higher energy than the excited QD) and block all the background light from the excitation laser. The cavity-emission signal is then sent to a single-photon counter, followed by a picosecond time analyzer (PTA) with a time resolution of ∼100 ps. The PTA is triggered by the excitation-laser pulse, and the cavity emission is recorded. Figure 3 shows the pulse shape (reflected from the semiconductor sample to show the delay and distortion of the pulse itself due to the setup and the PTA) as well as the rising and falling edges of the cavity emission for different temperatures. By fitting exponentials to the cavity signal, we estimate the fall times of the cavity emission. In practice, both the rise and fall times are complicated functions of the dipole-decay rate γ, the phonon-coupling rate γ_r, and the cavity-decay rate κ. From a simple rate-equation calculation (where the population goes from the QD to the cavity with a rate γ_t), under the assumption that all the population is in the QD excited state at time zero, we can find that the cavity population is proportional to $e^{-(\gamma_t+\gamma)t} - e^{-\kappa t}$ (see the Appendix). Under the assumption that the QD and the cavity operators are uncorrelated, mean-field equations derived from the master equation show that the rate of transferring population from the QD to the cavity is given by $\gamma_t = \langle\sigma^\dagger\sigma\rangle\gamma_r$ (where $\langle\sigma^\dagger\sigma\rangle$ is the QD-excited-state population), making the rate equations nonlinear. However, the transfer happens only when the QD is in the excited state, i.e., $\langle\sigma^\dagger\sigma\rangle \approx 1$. Hence, to simplify, we use a constant γ_t in the rate equations. In our system, the cavity-decay rate κ is an order of magnitude larger than both γ and γ_t, and the fall time of the cavity emission mainly follows $e^{-(\gamma_t+\gamma)t}$. We fit the fall time of the cavity emission with an exponential and find a value of ∼850 ps, showing $(\gamma + \gamma_t)/2\pi \sim 0.2$ GHz. From independent measurements, we know that the radiative QD lifetime is $1/\gamma \sim 5$ ns when the QD is not Purcell enhanced and in the photonic band gap.[31] From this, we can estimate $\gamma_t/2\pi \sim 0.15$ GHz. We note that the QD lifetime depends on the QD size and growth process, and hence, only an order of magnitude estimation of these rate parameters can be obtained. The QD in this particular case is red detuned from the cavity, so to have off-resonant coupling, a phonon needs to be absorbed. The temperature is changed from 40 K to 50 K, corresponding to a change in dot-cavity detuning from 1.8 nm to 2.25 nm and a change in mean phonon number $\bar{n}$ only from 7.8 to 8.[27] Hence, the slight difference between the fall times cannot be attributed to the increase in phonon density.

IV. COUPLING BETWEEN TWO QUANTUM DOTS

In this section, we present experimental data showing dot-to-dot coupling via an off-resonant cavity for two different systems: one with a strongly coupled QD and the other with a weakly coupled QD. In the first system, we excite the higher-energy QD2 resonantly with a laser and observe emission both from the lower-energy off-resonant cavity and QD1 (Fig. 4). Note that QD1 is strongly coupled to the cavity, and we observe anticrossing between the cavity and QD1 in

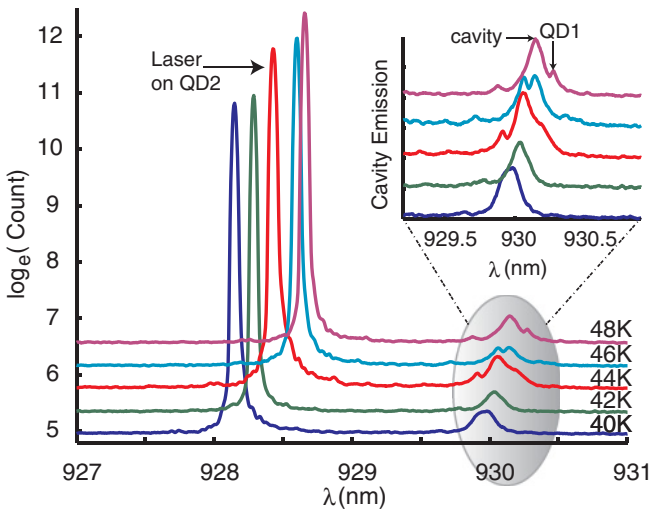

FIG. 4. (Color online) Measurement of the emission from the off-resonant cavity and QD1 under resonant excitation of QD2. We observe anticrossing between QD1 and the cavity when the temperature of the system is changed. The natural log of the count from the spectrometer charge-coupled device (CCD) is plotted. The inset zooms into the cavity emission, showing the anticrossing between QD1 and the cavity. The plots are vertically offset for clarity.

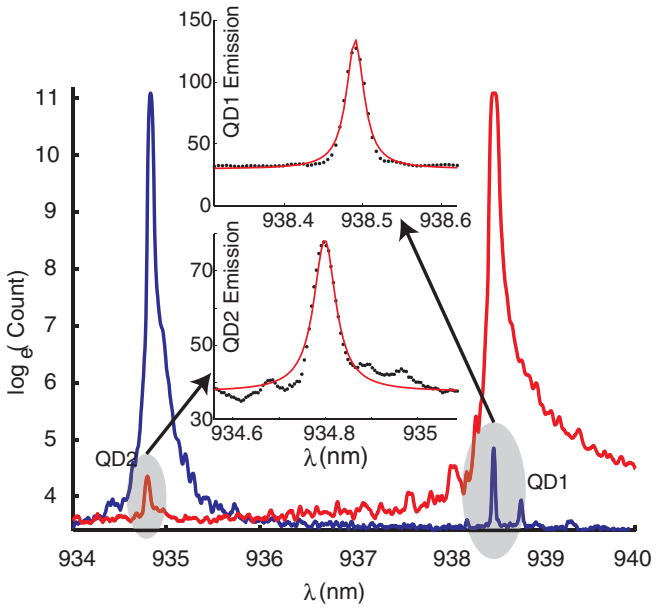

FIG. 5. (Color online) Experimental demonstration of the phonon-mediated interdot coupling. We observe the emission from the lower-energy QD1 when the higher-energy QD2 is resonantly excited (blue). Similarly, under resonant excitation of the lower-energy QD1, emission from the higher-energy QD2 is observed (red). Natural log of the count from the spectrometer CCD is plotted. The inset zooms into the QD emission (the actual spectrometer CCD counts are plotted). QD linewidths are estimated by fitting Lorentzians. Measured linewidths of the higher- and lower-energy QDs, respectively, are ∼0.03 nm and ∼0.013 nm. The cavity is at ∼935 nm, close to the higher-energy QD2.

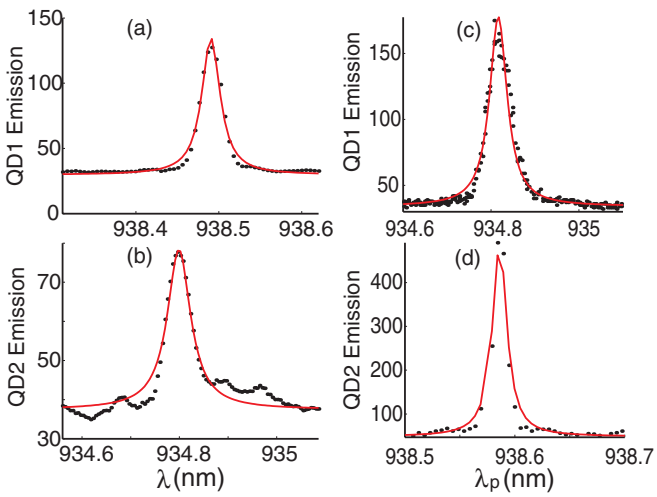

FIG. 6. (Color online) Comparison of the linewidths measured in direct off-resonant dot emission (Fig. 5) and from resonant spectroscopy of the QDs. (a),(b) The off-resonant QD emission (same as the inset of Fig. 5). QD linewidths are estimated by fitting Lorentzians. Linewidths of the higher- and lower-energy QDs, respectively, are ∼0.03 nm and ∼0.013 nm. The cavity is at ∼935 nm, close to the higher-energy QD. (c),(d) The off-resonant dot emission as a function of the pump-laser wavelength λ_p. In this experiment, a laser is scanned across one QD, and emission is collected from the other QD as a function of the laser wavelength as in Ref. 32. By fitting Lorentzians, we estimate the linewidths of the higher- and lower-energy QDs to be ∼0.024 nm and ∼0.008 nm, respectively. The y axis plots the photon counts obtained in the spectrometer CCD.

the off-resonant emission when the temperature of the system is changed (see inset of Fig. 4). The experimental data match well qualitatively with the theoretical result shown in Fig. 2(a). The emission from QD1 diminishes as QD1 is detuned from the cavity, showing that the coupling between the two dots is enhanced by the presence of the cavity, and g_2 has an important contribution. However, when we scan the pump laser across the lower-energy QD1 and observe the higher-energy-QD2 emission in this system, we obtain the cavity linewidth showing the usual cavity-to-QD2 coupling.[32] This might be due to the high temperature (40–48 K) of the system as will be explained later in this paper.

In the second system, the higher-energy QD2 that is spectrally close to the cavity is only weakly coupled to it. We observe emission from the lower-energy QD1 when a laser resonantly excites the higher-energy QD2 (see the blue plot of Fig. 5). We also observe up-conversion, i.e., emission from the higher-energy QD2 under excitation of the lower-energy QD1 (see the red plot of Fig. 5). The energy difference between the two QDs corresponds to a 1.2-THz acoustic phonon. The cavity is at ∼935 nm, closer to the higher-energy QD2, although its emission is not distinctly noticeable. The data is taken at 25 K. In the inset of Fig. 5 [replicated in Figs. 6(a) and 6(b)], we plot the collected emission from the QD which is not resonant with the laser and estimate the linewidth by a Lorentzian fit. The higher- and lower-energy QDs, respectively, have linewidths of ∼0.03 nm and ∼0.013 nm. These are comparable to the linewidths of the self-assembled QDs[32] and indicate that the coupling is indeed between two QDs. The broader linewidth of the higher-energy QD is due to the presence of the cavity. Following this, we perform a more accurate measurement of the linewidths of each QD by observing the peak amplitude of the emission from the off-resonant dot as a function of the pump-laser wavelength λ_p [Figs. 6(c) and 6(d)], giving us an estimate for the linewidth of the other (resonantly excited) QD, as the laser scans across it.[32] From the Lorentzian fit, we estimate that linewidths of the higher- and lower-energy QDs are, respectively, ∼0.024 nm and ∼0.008 nm. The slightly smaller linewidths measured by the latter approach are due to the better spectral resolution offered by this method.[32]

Finally, we performed a study of the effects of temperature on the interdot coupling. We note that while down-conversion of the pump light is observed at a temperature as low as 10 K, we did not observe any up-conversion at this temperature. This corroborates the fact that the observed dot-to-dot coupling is phonon mediated, and at low temperatures, up-conversion cannot happen due to the smaller number of phonons. We first scan the laser across the higher-energy QD and observe the off-resonant emission from the lower-energy QD. Figure 7(a) shows the result of this measurement for a set of different temperatures. Similarly, Fig. 7(b) shows the data obtained by scanning the laser across the lower-energy QD and observing the off-resonant emission from the higher-energy QD for an assortment of temperatures. The cavity is spectrally closer to

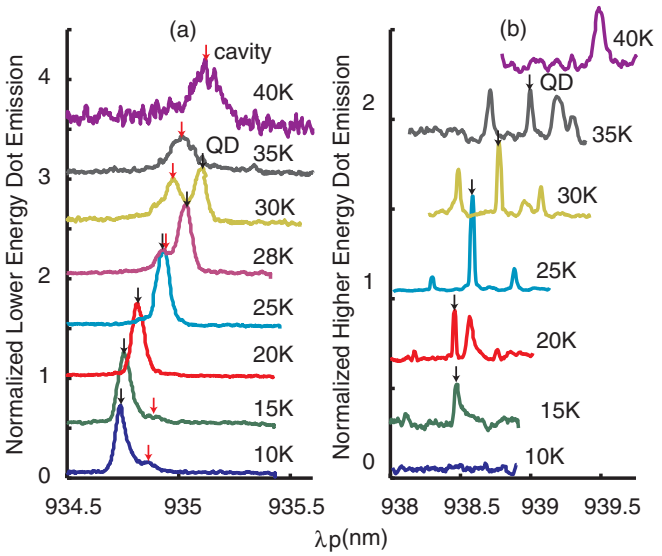

FIG. 7. (Color online) Effects of temperature on dot-to-dot coupling and the resulting frequency conversion of the pump. In the experiments, the wavelength of the pump λ_p is scanned through one QD, and the peak intensity of the other QD is monitored. (a) The pump is scanned through the higher-energy QD, and the down-converted light from the lower-energy QD is collected and plotted. (b) We plot the up-converted light emitted from the higher-energy QD as the pump is scanned through the lower-energy QD. All plots are separately normalized by the maximum QD-emission intensity in each plot and are vertically offset for clarity.

the higher-energy QD. It can be seen from the down-conversion plots in Fig. 7(a) that at lower temperatures we observe emission from the lower-energy QD only when the pump is within the linewidth of the higher-energy QD (the QD of interest and the cavity are shown by arrows). Up to 25 K, the coupling is mostly between the two QDs: the emission from the lower-energy QD is collected only when the higher-energy QD is excited, and the linewidth measured is closer to a QD linewidth. However, with increasing temperature (28 K and higher), we observe emission from the lower-energy QD even when the cavity is pumped. When the temperature is raised to ∼40 K, we observe coupling only from the cavity to the lower-energy QD (i.e., emission from the lower-energy QD is collected only by exciting the cavity and not by exciting the higher-energy QD), similar to the observations reported previously.[6] The disappearance of the dot-to-dot coupling (while preserving off-resonant cavity-to-dot coupling) is also noticed in Fig. 4 (for the system with only a strongly coupled dot and at 45 K temperature). This effect might be caused by the increase in phonon density and the resulting broadening of the QD lines. In Fig. 7(b), we monitor the effects of temperature on the up-conversion (the QD of interest is shown by an arrow). We cannot detect the up-conversion at 10 K as it only becomes observable at higher temperatures. However, with increasing temperature, the QD lines disappear. This is most likely due to the fact that the QD starts losing confinement at higher temperatures. The additional peaks in Fig. 7(b) show up-conversion of several other QDs.

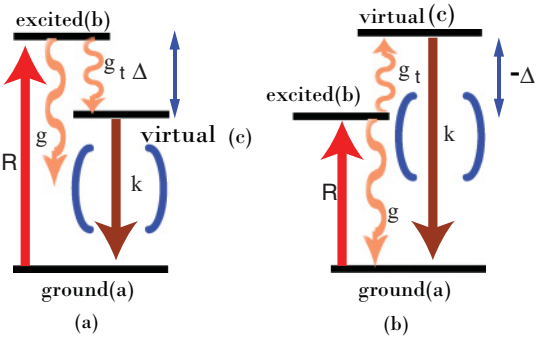

FIG. 8. (Color online) Simple level diagrams of the off-resonantly coupled-QD-cavity system for a (a) blue and (b) red detuned QD. The ground state a and excited state b of the QD are coupled via a laser. The excited state can decay to the ground state with a rate γ and to the virtual state with a rate γ_t. The cavity couples the virtual state to the ground state, and the cavity-decay rate is κ. In our experiment we measure the population in the virtual state or $c(t)$.

V. CONCLUSION

In summary, we observed phonon-mediated interdot coupling, both in systems with strongly and weakly coupled QDs. Both frequency up- and down-conversion were reported via a phonon of estimated frequency ∼1.2 THz. Our results indicate that this coupling is enhanced by the presence of the cavity, and that without a cavity spectrally close to one of the QDs, this process does not occur.

ACKNOWLEDGMENTS

The authors acknowledge financial support provided by the Office of Naval Research (PECASE Award), NSF, and ARO. E.K. acknowledges support from the IC Postdoctoral Research Fellowship. A.R. was supported by a Stanford Graduate Fellowship. The authors acknowledge Pierre Petroff and Hyochul Kim for providing the QD sample.

APPENDIX: RATE EQUATIONS

The rate equations describing the dynamics of the coupled-QD-cavity system (Fig. 8) are given by

$$\frac{da}{dt} = \gamma b + \kappa c - R(t), \tag{A1}$$

$$\frac{db}{dt} = R(t) - (\gamma + \gamma_t)b, \tag{A2}$$

$$\frac{dc}{dt} = \gamma_t b - \kappa c. \tag{A3}$$

As in our experiment, we are mainly measuring the emission from the cavity [i.e., the $c(t)$] after the pump excites the QD. $a(t)$ and $b(t)$ are populations of the QD ground and excited states, respectively (see Fig. 8). These equations can be rewritten as a second-order differential equation for $c(t)$

$$\frac{d^2c}{dt^2} + (\gamma + \gamma_t + \kappa)\frac{dc}{dt} + \kappa(\gamma + \gamma_t)c = \gamma_t R(t). \tag{A4}$$

Assuming the excitation pulse is a delta function $R(t) = R_o\delta(t)$, we find the cavity output in the frequency domain as

$$c(s = i\omega) = \frac{R_o\gamma_t}{s^2 + s(\kappa + \gamma + \gamma_t) + \kappa(\gamma + \gamma_t)} \quad \text{(A5)}$$

$$= \frac{R_o\gamma_t}{(s + \kappa)(s + \gamma + \gamma_t)} \quad \text{(A6)}$$

$$= \frac{R_o\gamma_t}{\kappa - \gamma - \gamma_t}\left(\frac{1}{s + \gamma + \gamma_t} - \frac{1}{s + \kappa}\right). \quad \text{(A7)}$$

Approximating $R(t)$ by a delta function is valid for our experiment as the duration of the pulse used is 3 ps whereas the QD lifetimes are on the order of nanoseconds and the cavity lifetime is ~50 ps. Taking an inverse Laplace transformation, we find $c(t)$. With the initial conditions $c(0) = 0$ and $\frac{dc}{dt}|_{t=0} > 0$, the solution is given by $c(t) = \frac{R_o\gamma_t}{\kappa-\gamma-\gamma_t}(e^{-(\gamma_t+\gamma)t} - e^{-\kappa t})$ for $\kappa > (\gamma + \gamma_t)$.

*arkam@stanford.edu

[1] K. Hennessy, A. Badolato, M. Winger, D. Gerace, M. Atature, S. Gulde, S. Falt, E. L. Hu, and A. Imamoglu, Nature (London) **445**, 896 (2007).

[2] D. Press, S. Götzinger, S. Reitzenstein, C. Hofmann, A. Löffler, M. Kamp, A. Forchel, and Y. Yamamoto, Phys. Rev. Lett. **98**, 117402 (2007).

[3] M. Kaniber, A. Laucht, A. Neumann, J. M. Villas-Boas, M. Bichler, M.-C. Amann, and J. J. Finley, Phys. Rev. B **77**, 161303(R) (2008).

[4] D. Dalacu, K. Mnaymneh, V. Sazonova, P. J. Poole, G. C. Aers, J. Lapointe, R. Cheriton, A. J. SpringThorpe, and R. Williams, Phys. Rev. B **82**, 033301 (2010).

[5] A. Laucht, N. Hauke, A. Neumann, T. Günthner, F. Hofbauer, A. Mohtashami, K. Müller, G. Böhm, M. Bichler, M.-C. Amann *et al.*, J. Appl. Phys. **109**, 102404 (2011).

[6] D. Englund, A. Majumdar, A. Faraon, M. Toishi, N. Stoltz, P. Petroff, and J. Vučković, Phys. Rev. Lett. **104**, 073904 (2010).

[7] S. Ates, S. M. Ulrich, A. Ulhaq, S. Reitzenstein, A. Löffler, S. Höfling, A. Forchel, and P. Michler, Nat. Photonics **3**, 724 (2009).

[8] U. Hohenester, Phys. Rev. B **81**, 155303 (2010).

[9] U. Hohenester, A. Laucht, M. Kaniber, N. Hauke, A. Neumann, A. Mohtashami, M. Seliger, M. Bichler, and J. J. Finley, Phys. Rev. B **80**, 201311 (2009).

[10] S. Hughes, P. Yao, F. Milde, A. Knorr, D. Dalacu, K. Mnaymneh, V. Sazonova, P. J. Poole, G. C. Aers, J. Lapointe *et al.*, Phys. Rev. B **83**, 165313 (2011).

[11] J. Suffczyński, A. Dousse, K. Gauthron, A. Lemaitre, I. Sagnes, L. Lanco, J. Bloch, P. Voisin, and P. Senellart, Phys. Rev. Lett. **103**, 027401 (2009).

[12] I. Wilson-Rae and A. Imamoğlu, Phys. Rev. B **65**, 235311 (2002).

[13] F. Milde, A. Knorr, and S. Hughes, Phys. Rev. B **78**, 035330 (2008).

[14] M. Winger, T. Volz, G. Tarel, S. Portolan, A. Badolato, K. J. Hennessy, E. L. Hu, A. Beveratos, J. Finley, V. Savona *et al.*, Phys. Rev. Lett. **103**, 207403 (2009).

[15] N. Chauvin, C. Zinoni, M. Francardi, A. Gerardino, L. Balet, B. Alloing, L. H. Li, and A. Fiore, Phys. Rev. B **80**, 241306(R) (2009).

[16] M. Calic, P. Gallo, M. Felici, K. A. Atlasov, B. Dwir, A. Rudra, G. Biasiol, L. Sorba, G. Tarel, V. Savona *et al.*, Phys. Rev. Lett. **106**, 227402 (2011).

[17] A. Majumdar, A. Papageorge, E. D. Kim, M. Bajcsy, H. Kim, P. Petroff, and J. Vučković, Phys. Rev. B **84**, 085310 (2011).

[18] R. Bose, D. Sridharan, G. S. Solomon, and E. Waks, Appl. Phys. Lett. **98**, 121109 (2011).

[19] A. Laucht, J. M. Villas-Bôas, S. Stobbe, N. Hauke, F. Hofbauer, G. Böhm, P. Lodahl, M.-C. Amann, M. Kaniber, and J. J. Finley, Phys. Rev. B **82**, 075305 (2010).

[20] E. del Valle, F. P. Laussy, F. Troiani, and C. Tejedor, Phys. Rev. B **76**, 235317 (2007).

[21] F. P. Laussy, A. Laucht, E. del Valle, J. J. Finley, and J. M. Villas-Bôas, Phys. Rev. B **84**, 195313 (2011).

[22] A. N. Poddubny, M. M. Glazov, and N. S. Averkiev, Phys. Rev. B **82**, 205330 (2010).

[23] P. C. Cárdenas, N. Quesada, H. Vinck-Posada, and B. A. Rodrguez, J. Phys.: Condens. Matter **23**, 265304 (2011).

[24] K. J. Xu and C. Piermarocchi, Phys. Rev. B **84**, 115316 (2011).

[25] E. Gallardo, L. J. Martinez, A. K. Nowak, D. Sarkar, H. P. van der Meulen, J. M. Calleja, C. Tejedor, I. Prieto, D. Granados, A. G. Taboada *et al.*, Phys. Rev. B **81**, 193301 (2010).

[26] E. B. Flagg, J. W. Robertson, S. Founta, W. Ma, M. Xiao, G. J. Salamo, and C.-K. Shih, Phys. Rev. Lett. **102**, 097402 (2009).

[27] A. Majumdar, E. D. Kim, Y. Gong, M. Bajcsy, and J. Vučković, Phys. Rev. B **84**, 085309 (2011).

[28] C. Roy and S. Hughes, Phys. Rev. Lett. **106**, 247403 (2011).

[29] S. M. Ulrich, S. Ates, S. Reitzenstein, A. Loffler, A. Forchel, and P. Michler, Phys. Rev. Lett. **106**, 247402 (2011).

[30] D. Englund, A. Faraon, I. Fushman, N. Stoltz, P. Petroff, and J. Vučković, Nature (London) **450**, 857 (2007).

[31] D. Englund, D. Fattal, E. Waks, G. Solomon, B. Zhang, T. Nakaoka, Y. Arakawa, Y. Yamamoto, and J. Vučković, Phys. Rev. Lett. **95**, 013904 (2005).

[32] A. Majumdar, A. Faraon, E. D. Kim, D. Englund, H. Kim, P. Petroff, and J. Vučković, Phys. Rev. B **82**, 045306 (2010).